ISSN 2395-1621

# Finite element analysis of carbon nanotube based composites

[#1]Mr. B. M. Powar, [#2]Mr. S. M. Sanap

bharatpowar07@gmail.com
sanapsunil@gmail.com

[1]Appearing M.E. (Design),
Department of Mechanical Engg.
Sinhgad Academy of Engg. Kondhwa(BK), Pune.
Maharashtra, India
[2]Assistant Professor,
Department of Mechanical Engg.
Sinhgad Academy of Engg. Kondhwa(BK), Pune.
Maharashtra, India

**ABSTRACT**

**In CNT based composites one or more CNTs may break due to different reasons and it is possible that a CNT based composite is having broken CNTs in it. Therefore it is important to understand the influence of such broken CNT in the nanocomposites in terms of stress redistribution and possibilities of failure. Present study deals with studying the effect of a broken CNT in the composite in the form of normal and shear stress redistribution surrounding the broken CNT in a CNT-based composite. Near broken CNT small debonding between CNT and matrix has been considered as a crack. At the crack front stresses responsible for three modes of fracture have been studied and stress distributions ahead of crack front along the interface of CNT and matrix has been found. Components of strain energy release rates (SERR) responsible for three modes of fracture are also calculated using virtual crack closure integral technique (VCCT). It has also been found that the debonding between CNT and matrix is due to pure mode II component of stress and mode I and mode II stress components does not contribute to the debonding. Effect of volume fraction on stress distribution and on strain energy release rate has also been studied.**

**Keywords— CNT-Based Composites, Stress Distribution, Strain Energy Release Rate, Virtual Crack Closure Integral.**

ARTICLE INFO

**Article History**

Received :18th November 2015

Received in revised form :

19th November 2015

Accepted : 21st November , 2015

**Published online :**

**22nd November 2015**

## I. INTRODUCTION

Composite material consists of two or more constituents/materials (or phases), designed to improve the overall mechanical properties.In general all composites have two or more constituents, in which the constituent that is continuous in the composite is called as the matrix. The basic idea of the composite is to optimize material properties of the composite, i.e., the properties of the matrix are to be improved by incorporating the reinforcement phase or reinforcement such as fiber, particles or flakes. In general, fibers are the principal load-carrying constituents while the surrounding matrix just helps to keep them in desired location and orientation and also act as a load transfer medium between them. Examples of composite materials are Concrete, Glass fiber reinforced plastic, Carbon nanotubes in polymer etc.

Carbon Nanotubes (CNTs)

Since the discovery of carbon nanotubes by Ijima in 1991 [1], they have excitedscientists and engineers in the research field. They are extremely small in size, having strengths 20 times that of high strength steel alloys and half as dense as aluminum. The diameter of CNT is in the nanometer range and their length can be in the micrometer range. Carbon nanotubes not only exhibit exceptionally high stiffness, strength and resilience but also possess superior electrical, thermal and mechanical properties. These nanotubes are also chemically inert and are able to sustain a high strain without breakage. These properties of CNTs are believed to be ideal for using them as reinforcements in high performance structural composites. Therefore, among many potential applications of nanotechnology, nanocomposites have been one of the latest research areas in the recent years and hence a large number of works has already been reported in the direction of modeling and characterization of CNTbased composites. Due to their extremely small sizes, analytical models are difficult to be established, fabrication process and tests are extremely difficult and expensive to conduct. On the other hand, modeling and simulation can be advantageously used to analyze such Nano composites. In spite of all the advantages, sometimes the CNT-based composites may have one or more CNTs.

Details of Carbon Nanotubes(CNTs) :

In general, CNTs are classified as

1. Single-walled carbon nanotubes (SWNTs):A SWNT is a hollow structure formed by covalently bonded carbon atoms and can be imagined as a thin graphene sheet rolled into a cylindrical shape. The CNTs can be sealed at both the ends using end caps, generally called as hemispherical caps. If the end caps are neglected the focus is on the large aspect ratio of the cylinder (i.e., length to diameter ratio as large as ($10^4$-$10^5$) which in general are called as long/continuous CNTs. These SWNTs typically have diameters ranging from 0.7-5.0 nm with thickness of 0.34 nm.

2.Multi-walled carbon nanotubes (MWNTs): MWNT have a number of graphene sheets co-axially rolled together to form a cylindrical tube consisting of 2-50 of these tubes and has inner diameters of 1.5–15.0 nm and outer diameters of 2.5- 30.0 nm (see Figure 1.1). Depending on the angle at which the graphite sheet is rolled, armchair, zigzag or chiral nanotubes are formed (see Figure 1.2)shows the different types of CNTs formed from a hexagonal graphemesheet. If the rectangle (ABCD) is cut from the graphene sheetand rolled up in such a way that the tip (B) of the chiral vector($C_h$) touches its tail (A), chiral CNT is produced.

$$C_h = n\,a_1 + m\,a_2 \qquad (1.2)$$

Where the integers (n, m) are the number of steps along the zigzag carbon bonds and $a_1$ and $a_2$are unit vectors as shown in Figure 1.

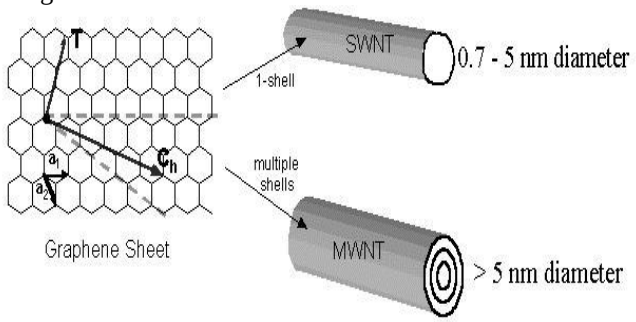


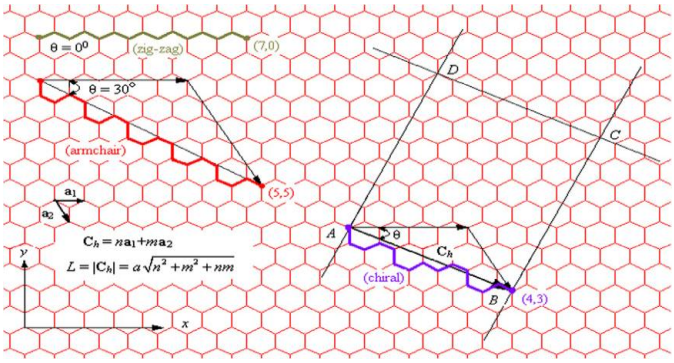


Figure **Error! No text of specified style in document.**: Formation of different types of CNTs [zigzag (7, 0), armchair (5, 5) and chiral (4, 3)] by rolling up a hexagonal graphene shee

## II. LITERATURE REVIEW

Carbon nanotubes are fullerene-related structured discovered by a Japanese electron microscopistIijimaS. [1] which consists of multi-graphene cylinders closed at either end with caps containing pentagonal rings by a direct current arc discharge between carbon electrodes immersed in helium gas under a temperature of 3000 degree centigrade, the MWCNT were created. Liu &Chen [2] determined the elastic and mechanical properties of CNTs using 3-D nanoscale representative volume elementusing FEM. They derived the formulas to extract effective material constants from solutions for RVE under three loading cases. They proved that with 2% and 5% volume fractions of CNTs in matrix, the stiffness of the composite in the CNT axial direction can increase as much as 0.7 and 9.7 times for the case of short and long CNT fibers, respectively. SushenKirtania and Debabrata Chakraborty [30] studied the stress distribution in the vicinity of broken CNT in CNT-reinforced composites. They performed three-dimensional finite element analysis using multiscale modeling considering a square RVE containing 9 CNTs and studied the effect of broken CNT on the adjacent CNTs and on the matrix for CNT/Epoxy and CNT /Titanium composites. They analyzed the stress distribution in broken CNT, at the interface, and in the adjacent CNTs for different volume fractions. SushenKirtania and Debabratachakraborty [44] studied the debonding between broken CNT and matrix in CNT based composites. They have performed a full 3D finite element analysis with multi scale modeling. A square RVE with one CNT surrounded by matrix was considered. They have used contact elements between CNT and matrix to study the debonding around the fiber break and determined the strain energy release rates using virtual crack closure integral technique. Literature review reveals that a good number of papers are available in the field of finite element analysis of CNT based composites mostly in characterization of such composites. However, there is not much work in the area of analysis of broken fiber for CNT composites. Even though some works [16, 18, and 19] are there, they have considered finite element analysis using a continuous CNT. Kirtania and Chakraborty [30], [44] have studied the failure analysis of CNT composites in details.

## III.EXPERIMENTATION

In the part of experimentation various types of steps or parts are included as:

ANSYS software has been used for 3D modeling of CNT based composites. Element used to create mesh is SOLID45. This element is defined by eight nodes having three degrees of freedom $(u, v, w)$ at each node: translations in the nodal x, y, and z directions. The element has plasticity, creep, swelling, stress stiffening, large deflection, and large strain capabilities.

Finite element modeling of a RVE for CNT-reinforced composites containing broken CNT

A square RVE having singleCNT in the matrix has been considered for the analysis. Most of the literatures have considered the linear behavior of CNTs in CNT-based composites. But in reality for larger deformation, CNTs behave nonlinearly and the nonlinear behavior of CNT is considered for the present analysis.

The stress–strain curves of the armchair and zigzag CNTs were found experimentally by Tserpes et al. [22] and by fitting the data of the curves using third order polynomials, they obtained following relations between the stress and strain.

$$\sigma_n = 2909.8\varepsilon_n^3 - 4995.6\varepsilon_n^2 + 1364.9\varepsilon_n \quad (3.5)$$

(for zigzag CNT)

$$\sigma_n = 5958.5\varepsilon_n^3 - 4769.4\varepsilon_n^2 + 1334.7\varepsilon_n \quad (3.6)$$

(for armchair CNT)

Equation (3.5) has been used in the present analysis considering zigzag CNT. The stress-strain curve data for the zigzag CNT as given by equation (3.5) has been inputted in to ANSYS. Epoxy and Copper have been chosen to study the effect of matrix materials on the stress distribution around the broken CNT in the CNT-based composites. Properties of matrix materialare as follows

For epoxy $E_m = 3.89$ GPa, $\nu_m = 0.37$

For copper $E_m = 120$ GPa , $\nu_m = 0.34$

For zigzag CNT Equation (3.5) has been used with $E_{nt} = 1310$ GPa, $\nu_{nt} = 0.28$

1) Full model Boundary Conditions:

Figure 3.4 shows the FE mesh of full model of a RVE in which CNT is broken.All the nodes at one end of the RVE i.e. at $z = 0$ are fully restrained including nodes belonging to the broken CNT. The axial mechanical loading of the nanocomposites is applied by a uniform displacement in the axial direction at the other end of the RVE i.e. at nodes at $z = L_a = 50$ nm, where $L_a$ is the axial length of the RVE. The displacement increment was chosen equal to 1% of the length of the RVE. The total applied strain in the axial direction is 15% of the total axial length of the RVE.Total number of nodes and elements are 38784 and 33600 respectively in this FE model.

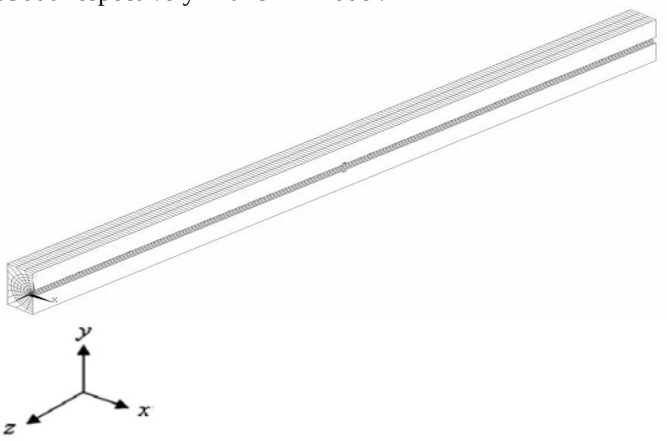


Figure 2: FE mesh of full model of CNT reinforced composite RVE (Sectional View)

Finite element modeling of a RVE for CNT-reinforced composites containing broken CNT with initial debonding

Figure 2 shows the pictorial view of 3D FE model with square RVE modeled in ANSYS where the x–y plane is the transverse plane and the z-axis is the axial direction. All the nodes at z = 0are fully restrained except the nodes belonging to the broken CNT and for the nodes at z = La=50 nm, where La is the axial length of the model, uniform displacement in the axial direction is applied. The displacement increment was chosen equal to 1% of the length of the RVE and the total applied strain in the axial direction is 7% of the total axial length of the RVE.

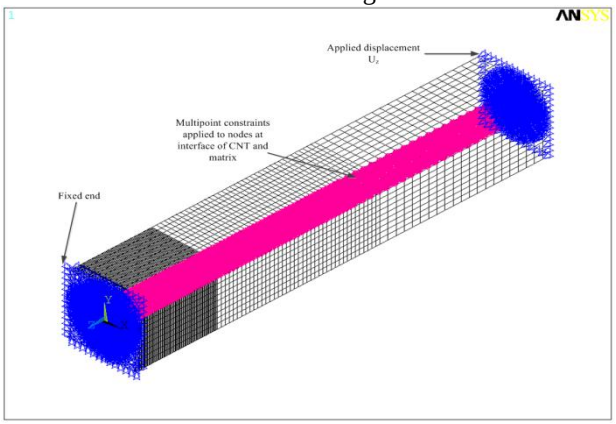


Figure 3: RVE for CNT-reinforced composites containing broken CNT with initial debonding

Initially it is assumed that near the CNT break there is a debonding between CNT and matrix and the length of the debonding in axial direction is considered as $a = 1$ nm. The virtual crack extension size is taken as $\Delta a = 0.2$ nm. Near the debonding or crack very fine mesh has been used. The length of the element in axial direction for first 10nm length of RVE is taken as 0.1 nm, for next 20 nm length of RVE it is taken as 0.5 nm and for the remaining 20 nm length of RVE lengths of elements is taken as 1 nm. The nodes which are placed at the interface of CNT and matrix have the same coordinates and are coupled through multi-point constraint equations. There are 7728 pairs of nodes at the interface of CNT and matrix which are having same coordinates and are coupled to each other using multipoint constraint equations in ANSYS. Total number of nodes and

elements are 156480 and 139968 respectively in this FE model.

Virtual crack closure technique (VCCT) to determine components of strain energy release rate.

Composites are material whose behavior is difficult to predict by using numerical methods especially in presence of damage. However, the finite element method used in conjunction with the Virtual Crack Closure Technique (VCCT) can provide effective information in terms of global behaviour of the structure in presence of an interfacial damage. The total SERR for a particular crack length can be obtained with separate finite element analysis of the problem, with two different crack lengths differing by a small amount Δa representing the virtual crack extension at each crack tip and estimating the difference in strain energy storedVCCT is one of the popular methods used for estimating both total and individual SERR components, evaluates these from a single finite element analysis based on Irwin's virtual crackclosure integral (VCCI) concept. This method is found to be simple and accurate, and is widely used for estimating mixed mode SERR components in interface crack problems.

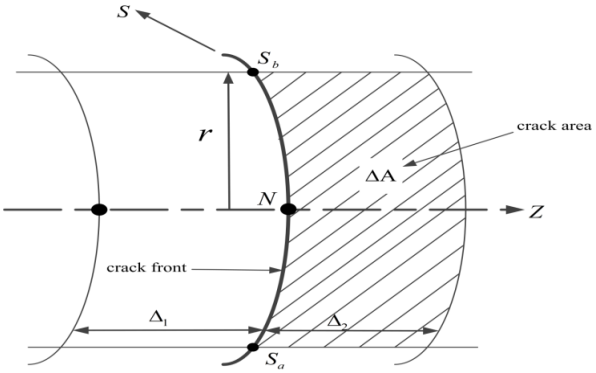


Figure 4 : 3D-VCCT model

In 3D-VCCT the nodal stress distribution at and ahead of the crack front, the displacement distribution behind the crack front and the virtual crack growth area just ahead of the front are required to calculate the components of SERR ($G_I, G_{II}, G_{III}$) at node N. 3D-VCCT is used in the present study to calculate the three components of SERR given by following equations.

$$G_I = \lim_{\Delta A \to 0} \frac{1}{2\Delta A} \int_{S_a}^{S_b} \int_{0}^{\Delta_2} \sigma_{rr}(z,s) u_r(\Delta_1, s) dz ds \quad (3.12)$$

$$G_{II} = \lim_{\Delta A \to 0} \frac{1}{2\Delta A} \int_{S_a}^{S_b} \int_{0}^{\Delta_2} \tau_{rz}(z,s) u_z(\Delta_1, s) dz ds \quad (3.13)$$

$$G_{III} = \lim_{\Delta A \to 0} \frac{1}{2\Delta A} \int_{S_a}^{S_b} \int_{0}^{\Delta_2} \tau_{rs}(z,s) u_s(\Delta_1, s) dz ds \quad (3.14)$$

And total strain energy release rate is given by

$$G_T = G_I + G_{II} + G_{III} \quad (3.15)$$

Out of all stress components, $\sigma_{rr}$ $\tau_{rz}$ and $\tau_{rs}$ are the main stress components due to which three modes of fracture occurs in the FE model. s. ΔA is the virtually closed crack area.

**Determination of axial normal stress distribution in the broken CNT and interfacial shear stress distribution at the interface of broken CNT and matrix**

In this section the axial normal stress of the broken CNT, interfacial shear stress at the interface of the broken CNT and matrix, of a square RVE with single CNT have been studied at a different volume fractions for CNT/Epoxy and CNT/Copper composites.

**2)** Axial normal stress in the broken CNT for CNT/Epoxy composites

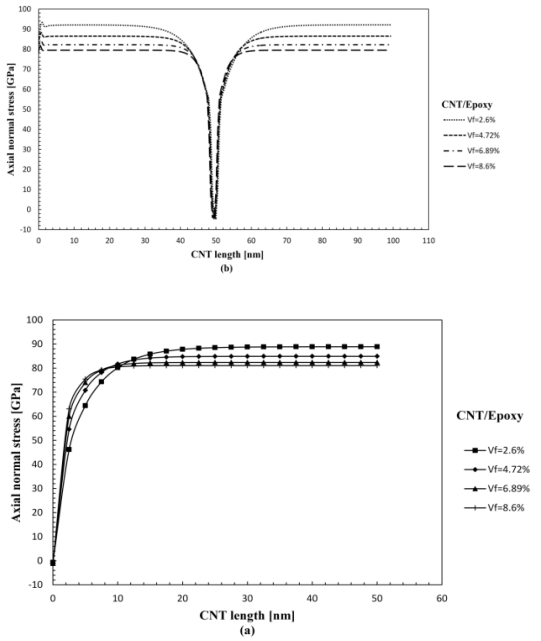


Figure 5:Variation of axial normal stress distribution in the broken CNT along the CNT length (a) Half model RVE (b) Full model RVE forCNT/Epoxy composite

**3) Interfacial shear stress at the interface of broken CNT and matrix for CNT/Epoxy composites**

Figure 5(a) and Figure 5(b) given below shows the variation of interfacial shear stress distribution at the interface of the broken CNT and matrix for half model RVE and full model RVE respectively for CNT/Epoxy composite. It could be observed that at the interface near the break, a high value of shear stress occurs indicating that CNT debonding or delamination may take place at that location. The magnitude of interfacial shear stress is 2.1 GPa for a CNT volume fraction of 2.6%.

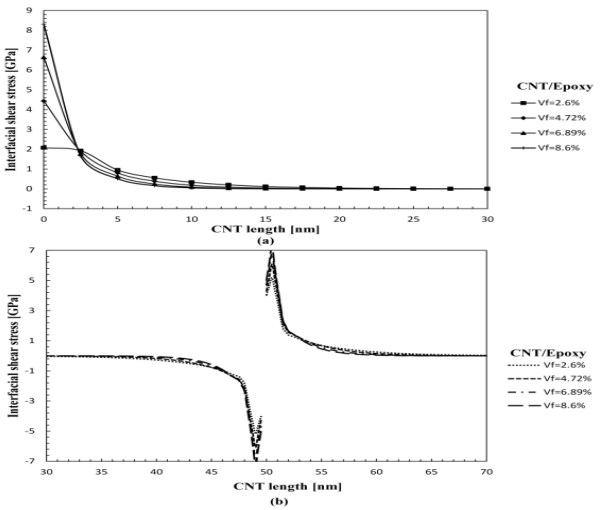


Figure 6:Variation of interfacial shear stress distribution at the interface of the broken CNT and matrix along the CNT length (a) Half model RVE (b) Full model RVE for CNT/Epoxy composite.

### 4) Effect of volume fraction on axial normal stress of broken CNT and interfacial shear stress for CNT/Epoxy composites

From Figure 6(a) the ineffective length of the broken CNT in CNT/Epoxy composites is 15 nm, 13 nm, 12.5 nm and 11 nm corresponding to volume fraction of 2.6%, 4.72%, 6.89% and 8.6% respectively. Hence in the case of CNT/Epoxy composites the broken CNT is ineffective up to 30% of the length and hence it contributes very less to the load bearing of the composite. It is observed that the ineffective length of the broken CNT decreases with the increase in volume fraction for CNT/Epoxy composite. From Figure 6(a) it could be seen that the magnitude of the interfacial shear stress increases with the increase in volume fraction of CNT. The magnitudes of interfacial shear stress are 2.1 GPa, 4.43GPa, 6.64 GPa and 8.3 GPa corresponding to volume fractions of 2.6%, 4.72%, 6.89% and 8.6% respectively for CNT/Epoxy composites.

### 5) Axial normal stress in the broken CNT for CNT/Copper composites

Figure 7 (a) and Figure 7(b)given below shows the variation of the axial normal stress along the length of the broken CNT for half model RVE and full model RVE respectively for different volume fractions of CNT for CNT/Copper composites.It could be observed that the broken CNT regained the nominal stress value after a length of 4 nm for CNT/Copper composite for a volume fraction of 2.6%. Therefore, it could be concluded that the ineffective length of the broken CNT in CNT/Copper composites is 8% for a volume fraction of 2.6% whereas it was 30% for CNT/Epoxy composites for same volume fraction. Therefore the ineffective length of CNT/Copper composites is four times less than that of the CNT/Epoxy composites.

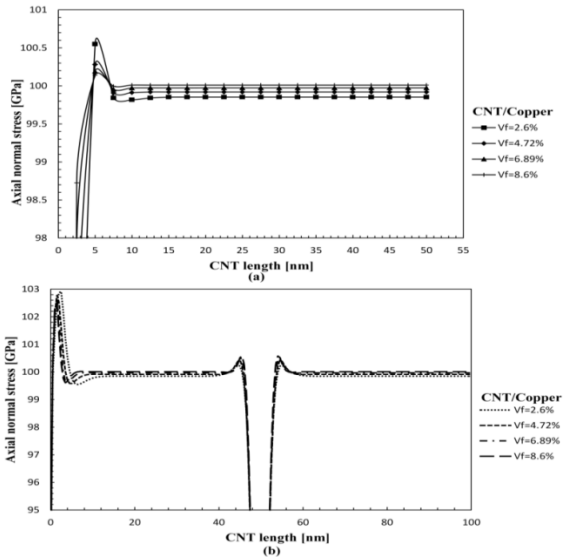


Figure 7: Variation of axial normal stress distribution in the broken CNT along the CNT length (a) Half model RVE (b) Full model RVE for CNT/Copper composite**.**

### 6) Interfacial shear stress at the interface of broken CNT and matrix for CNT/Copper composite

Figure 8 (a) and Figure 8(b) given below shows the variation of interfacial shear stress distribution at the interface of the broken CNT and matrix for half model RVE and full model RVE respectively for CNT/Copper composite.The magnitude of interfacial shear stress is 4.94 GPa for a CNT volume fraction of 2.6% whereas it was 2.1GPa for CNT/Epoxy composite for the same volume fraction.

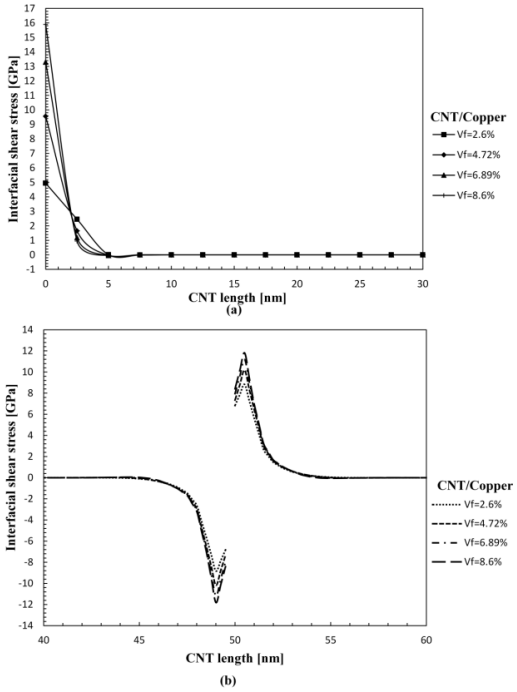


Figure 8: Variation of interfacial shear stress distribution at the interface of the broken fiber and matrix along the fiber length (a) Half model RVE (b) Full model RVE for CNT/Copper composites

**7) Effect of volume fraction on axial normal stress of broken CNT and interfacial shear stress for CNT/Copper composites**

From Figure 7(a) the ineffective length of the broken CNT in CNT/Copper composites is 4 nm, 3 nm, 2.5 nm and 2 nm corresponding to volume fraction of 2.6%, 4.72%, 6.89% and 8.6% respectively. Hence in the case of CNT/Copper composites the broken CNT is ineffective only up to 8% of the length and hence a major length of broken CNT contributes to the load bearing of the composite as compared to CNT/Epoxy composites (30% ineffective length). The ineffective length of the broken CNT decreases with the increase in volume fraction for CNT/Copper composite also.

From Figure 8 (a) it could be seen that the magnitude of the interfacial shear stress increases with the increase in volume fraction of CNT. The magnitudes of interfacial shear stresses are 4.94 GPa, 9.56GPa, 13.291 GPa and 15.897 GPa corresponding to volume fractions of 2.6%, 4.72%, 6.89% and 8.6% respectively for CNT/Copper composite. These values of interfacial shear stress of CNT/Copper composite are higher than that of the CNT/Epoxy composites for the same volume fraction. Therefore the chance of debonding at interface in CNT/Copper composites is higher than that in the CNT/Epoxy composites.

**Determination of stress distributions responsible for three modes of fracture and components of strain-energy release rate (SERR)**

From Figure 8 given in section 3.4 a representative volume element containing single CNT was considered for the analysis. CNT is considered as broken at one end anda small length of debonding between CNT and matrix in front of broken CNT is considered. The length of the debondingor crack at the interface in axial direction is considered as $a = 1$ nm.The virtual crack extension size was chosen Δa =0.2 nm. The debonding at the interface is considered over the entire circumference ahead of broken end of CNT for a length of 1 nm.The debonded area is equal to $2\pi r_0 a$ .This debonded area is the interfacial crack for the 3D square RVE. The virtual crack extension area is $\Delta A = 2\pi r_o \Delta a$ , where $\Delta a$ is the length of virtual crack extension in axial direction and $r_0$ is the outer radius of CNT. Multi-point constraint equations were used to model the crack in ANSYS.The totalapplied strain in the axial direction is 7% of the total axial length of the model.

**8) Stress distributions at the interface ahead of crack front for CNT/Epoxy composite for a constant volume fraction of 2.61%.**

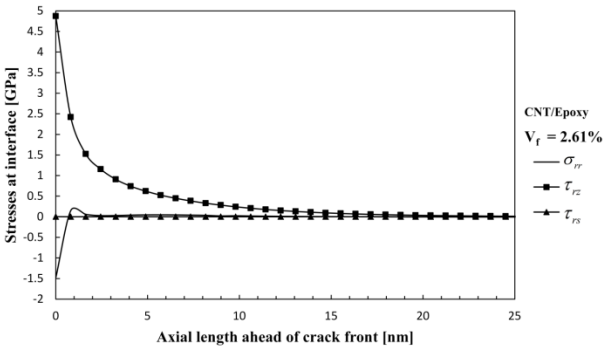


Figure 9: Stress distributions along the interface ahead of the crack front for a volume fraction of 2.61% for CNT/Epoxy composite.

From Figure 9 it have been observed that the value of interfacial normal stress $\sigma_{rr}$ is negative near the crack front (-1.5GPa)and it shows very small positive value (0.15 GPa) slightly away from the crack front and then reaches to zero for the remaining length of the interface but magnitude of negative stress dominates the magnitude of positive stress. Negative value of $\sigma_{rr}$ at the crack front signifies that it is a crack closing mode and hence it does not contribute to the debonding of CNT from epoxy. The magnitude of $\tau_{rz}$ is maximum (5.5 GPa) at the crack front and then reaches to zero after some length along the interface. The magnitude of $\tau_{rs}$ is nearly zero ahead of crack front for entire length of interface. From this result it is observed that high value of $\tau_{rz}$ exists near the crack front of CNT/Epoxy composite and negligible values of $\sigma_{rr}$ and $\tau_{rs}$ exists near the crack front hence only $\tau_{rz}$ (mode II stress) contributes to thedebonding of CNT from epoxy and other two stresses do not contribute to the debonding.

**9) Effect of volume fractions on stress distributions at the interface ahead of crack front for CNT/Epoxy composite**

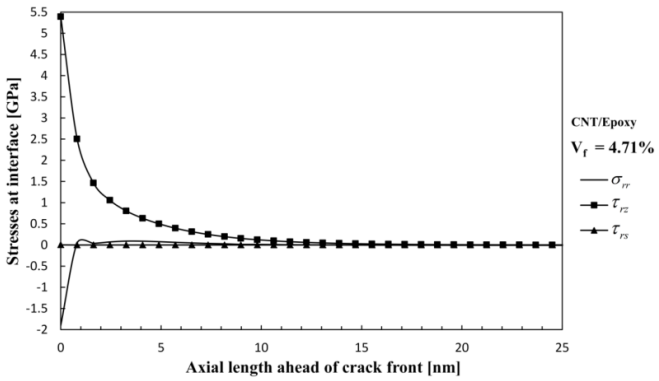


**(a)**

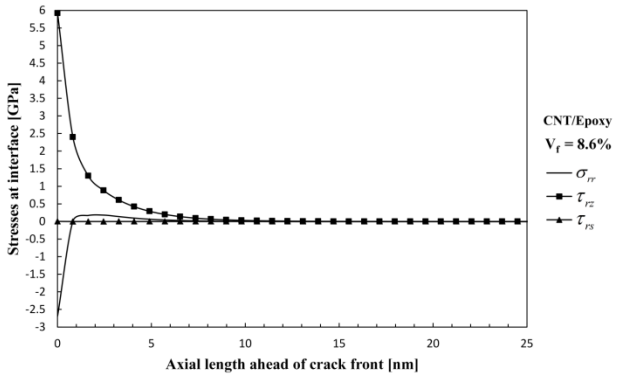


(b)

Figure 10: Distribution of stresses at interface ahead of crack front of CNT/Epoxy composites for a) CNT volume fraction of 4.71% b) CNT volume fraction of 8.6%.

From Figure 10 (a) and Figure 10(b) it is observed that the value of $\tau_{rz}$ near the crack front increases with increase in volume fraction for CNT/Epoxy composites. The values of $\tau_{rz}$ are 5.38 GPa and 6 GPa for the volume fractions of 4.71% and 8.6% respectively. The values of $\sigma_{rr}$ are -1.9 GPa and -2.7 GPa respectively for volume fractions of 4.71% and 8.6% respectively and it does not contribute to debonding. The magnitude of $\tau_{rs}$ is nearly zero ahead of crack front for entire length of interface for all volume fractions of CNT for CNT/Epoxy composites. The interfacial shear stress $\tau_{rz}$ is the only major component of stress which is responsible for debonding of CNT for CNT/Epoxy composites for all volume fractions of CNT.

**10) Stress distributions at the interface ahead of crack front for CNT/Copper composite for a constant volume fraction of 2.61%**

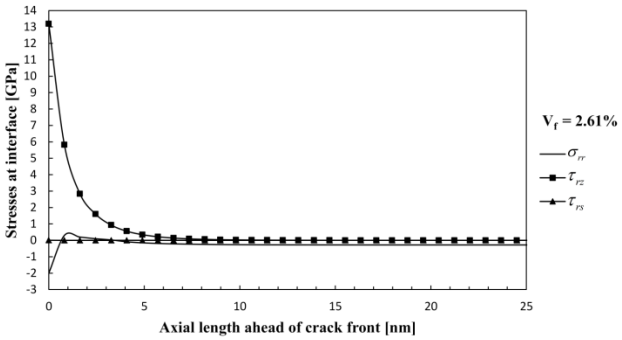


Figure 11: Stress distributions along the interface ahead of the crack front for a volume fraction of 2.61% for CNT/Copper composite.

From Figure 11 it is observed that the magnitude of $\tau_{rz}$ is 13.2 GPa at the crack front which is more than that of CNT/Epoxy (5.5 GPa) and then gradually reduces to zero along the interface at a CNT volume fraction of 2.61% for CNT/Copper composites.The value of interfacial normal stress $\sigma_{rr}$ is negative near the crack front (-2GPa) and it shows very small positive value (0.2GPa) slightly away from the crack front but magnitude of negative stress dominates the magnitude of positive stress therefore it is a crack closing mode and does not contribute to the debonding of CNT. The magnitude of $\tau_{rs}$ is nearly zero ahead of crack front for entire length of interface.From this result it is observed that high value of $\tau_{rz}$ exists near the crack front of CNT/Copper composite and negligible values of $\sigma_{rr}$ and $\tau_{rs}$ exists near the crack front hence only $\tau_{rz}$ (mode II stress) contributes to the debonding of CNT from copper and other two stresses do not contribute to the debonding.

**11) Effect of volume fractions on stress distributions at the interface ahead of crack front for CNT/Copper composite**

From Figure 12 (a) and Figure 12 (b) given below it is observed that the value of $\tau_{rz}$ near the crack front increases with increase in volume fraction for CNT/Copper composites also. The values of $\tau_{rz}$ are 14.5 GPa and 16.2 GPa for the volume fractions of 4.71% and 8.6% respectively. The values of $\sigma_{rr}$ are -2.7 GPa and -5.5 GPa respectively for volume fractions of 4.71% and 8.6% respectively and it does not contribute to debonding. The magnitude of $\tau_{rs}$ is nearly zero ahead of crack front for entire length of interface for all volume fractions of CNT for CNT/Copper composites. The interfacial shear stress $\tau_{rz}$ is the only major component of stress which is responsible for debonding of CNT for CNT/Copper composites for all volume fractions of CNT.

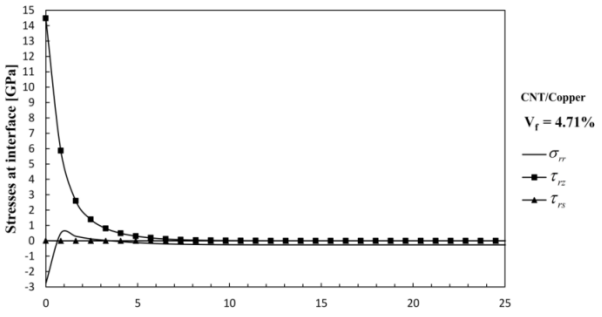


**(a)**

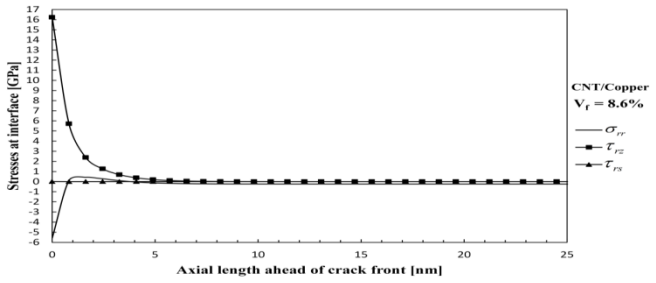


**(b)**

Figure 12: Distribution of stresses at interface ahead of crack front of CNT/Copper composites for a) CNT volume fraction of 4.71% b) CNT volume fraction of 8.6%.

**12) Determination of mode II component of strain-energy release rate ( $G_{II}$ ) and its variation along the circumference of crack front**

Since interfacial normal stress $\sigma_{rr}$ and interfacial shear stress $\tau_{rs}$ does not contribute to debonding of CNT the corresponding components of SERR $G_I$ and $G_{III}$ are negligible and as only interfacial shear stress $\tau_{rz}$ is significant near crack front, mode II component of SERR needs to be determined. The crack propagation mode is pure mode II. Equation (3.13) is used to determine $G_{II}$ . Figure 13 shows the variation of $G_{II}$ along the circular crack front for CNT/Epoxy and CNT/Copper composites for a constant volume fraction of 2.61%. It is observed that there is no variation of $G_{II}$ along the crack front for both CNT/Epoxy and CNT/Copper composites and value of $G_{II}$ for CNT/Epoxy is higher than value of $G_{II}$ for CNT/Copper composites. As values of $G_{II}$ are same for every node along the crack front its value can be found at any point along the crack front.

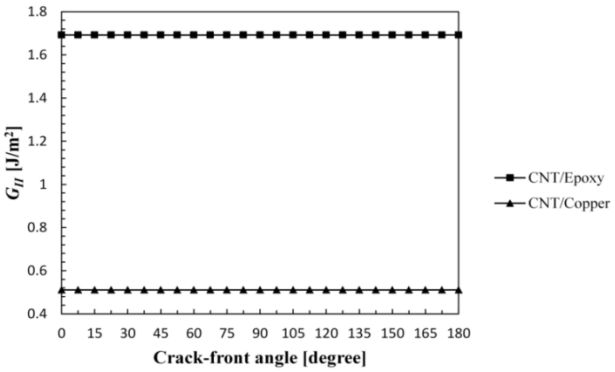


Figure 13: Variation of $G_{II}$ along the circular crack front for a volume fraction of 2.61% for CNT/Epoxy and CNT/Copper composites

**13) Variation of $G_{II}$ with volume fraction of CNT for CNT/Epoxy and CNT/Copper composite**

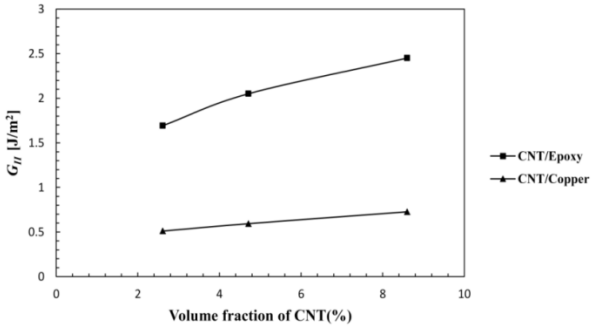


Figure 14: Variation of $G_{II}$ with volume fractions for CNT/Epoxy and CNT/Copper composites

Figure 14 shows the variation of $G_{II}$ with volume fractions for CNT/Epoxy and CNT/Copper composites. It could be observed that the values of $G_{II}$ are 1.69 J/m$^2$ and 0.51 J/m$^2$ for CNT/Epoxy and CNT/Copper composites respectively for a constant volume fraction of 2.61% therefore for a constant volume fraction of CNT the value of $G_{II}$ for CNT/Epoxy composites is 3.3 times higher than the value of $G_{II}$ for CNT/Copper composites. As volume fraction of CNT increases value of $G_{II}$ also increases. The value of $G_{II}$ is 2.05 J/m$^2$ and 2.45 J/m$^2$ for CNT/Epoxy composite for volume fractions of 4.71% and 8.6% respectively and for CNT/Copper composites value of $G_{II}$ is 0.6 J/m$^2$ and 0.72 J/m$^2$ for volume fractions of 4.71% and 8.6% respectively. The value of $G_{II}$ increases 1.45 times when the volume fraction is increased from 2.61% to 8.6% for CNT/Epoxy composites and this increase is 1.4 times when the volume fraction is increased from 2.61% to 8.6% for CNT/Copper composites.

**14) Stress distribution for CNT having hemispherical ends**

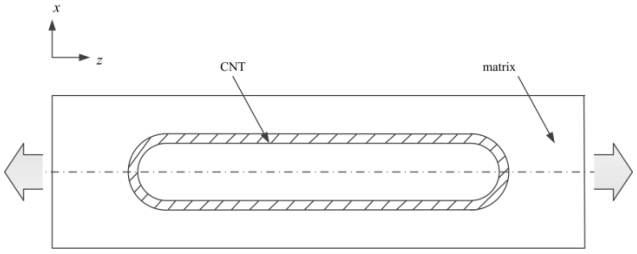


Figure 15: Axially loaded RVE containing CNT having hemispherical ends.

In reality CNTs are having hemispherical ends hence it is important to study stress distribution pattern for CNTs having hemispherical ends. Figure 4.12 shows the axially loaded RVE containing CNT having hemispherical ends. Axial normal stress distribution along CNT and interfacial shear stress distribution along interface of CNT/Epoxy composite for different l/d ratio has been obtained as shown in Figure 15 and Figure 16 respectively.

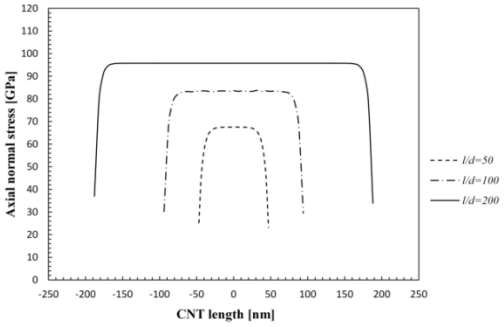


Figure 16: Axial normal stress distributions along CNT for different fiber lengths for CNT/Epoxy composites

From Figure 15 and Figure 16 it is observed that the uniform distribution of stresses can be attained in the middle section of CNT and stress variation occurs near the hemispherical ends. As length of the CNT increases the range of the uniform region also increases. For a very long

fiber the range of this uniform region can become sufficiently larger than non-uniform regions at the hemispherical ends. Thus the stresses in the uniform region are dominant compared to the non-uniform regions and a full stress transfer between the CNT and matrix is achieved. Near the hemispherical ends full stress transfer is not achieved but in the remaining portion of CNT full stress transfer is achieved between CNT and matrix.

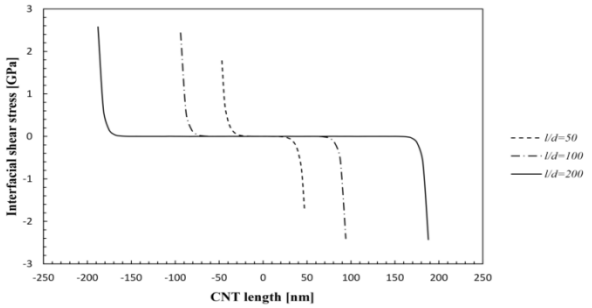


Figure 17: Interfacial shear stress distributions along interface of CNT/Epoxy composites for different fiber lengths

The variation of axial normal stress and interfacial shear stress for CNT having hemispherical ends obtained in the present work follows the same pattern as reported by H. Wan.

## IV. CONCLUSIONS

In the present study, the axial normal stress in the broken CNT, interfacial shear stress at the interface of the CNT and matrix for CNT reinforced composites have been studied using finite element modelling by considering a square RVE with single CNT also the stress distribution for CNTs having hemispherical ends has been studied. A small debonding near the broken CNT has been considered and distribution of stresses responsible for three modes of fracture near the crack front has been studied. The components of strain energy release rate have been determined for CNT reinforced composites using virtual crack closure integral technique. To study the effect of matrix material on the distribution of axial normal stress as well as interfacial stresses, two types of matrix materials viz. Epoxy and Copper have been chosen. Also the effect of volume fraction on stress distributions and strain energy release rate has been studied for CNT reinforced composites. The following conclusions aredrawn from the present study.

I. For CNT/Epoxy and CNT/Copper composites the ineffective length decreases with increase in volume fraction.

II. For both the CNT-based composites the magnitude of interfacial shear stress increases with increase in volume fraction of CNT.These values of interfacial shear stress for CNT/Copper composite are higher than that of the CNT/Epoxy composites for the same volume fraction. Therefore the chance of debonding at interface in CNT/Copper composites is higher than that in the CNT/Epoxy composites.

III. As only mode II component of stress $\tau_{rz}$ is responsible for debonding, mode II component of SERR $G_{II}$ needs to be determined and other two components $G_I$ and $G_{III}$ are negligible which shows that it is case of pure mode II debonding.

IV. Value of $G_{II}$ is constant along the circular crack front for both CNT/Epoxy and CNT/Copper composites.

V. Value of $G_{II}$ increases with increase in volume fraction of CNT for both CNT/Epoxy and CNT/Copper composites.The value of $G_{II}$ for CNT/Epoxy composites is 3.3 times higher than the value of $G_{II}$ for CNT/Copper composites for a constant volume fraction of CNT.

VI. For CNTs having hemispherical ends, full stress transfer is not achieved near the ends but in the remaining portion of CNT full stress transfer is achieved between CNT and matrix.

## REFERENCES

[1] S Iijima, “Helical microtubules of graphitic carbon”. Nature; vol.34, pp. 8–56, 1991.

[2] YJ Liu and XL Chen, “Evaluation of effective material properties of carbon nanotube-based composites using a nanoscale representative volume element,” Mechanics of material, vol 35, pp. 69-81, 2003.

[3] Li Chunyu and TW Chou, “A structural mechanics approach for the analysis of carbon nanotubes.” International Journal of Solids and Structures, vol. 40, pp.2487–2499, 2003.

[4] ] JR Xiao, BA Gama, JW Gillespie, “An analytical molecular structural mechanics model for the mechanical properties of carbon nanotubes.” International Journal of Solids and Structures, vol. 42 pp.3075–92, 2005

[5] ET Thostenson, Z Ren, TW Chou, “Advance in the science and technology of carbon nanotubes and their composites: a review,” Composite Science and Technology, vol 61, pp.1899–1912, 2001.

[6] S Kirtania, D Chakraborty, “Fracture behavior of carbon nanotube-based composites with a broken fiber using multi-scale finite element modeling,” Journal of Computational and Theoretical Nanoscience, vol. 11, pp.1-9, 2014.

[7] YL Chen, B Liu, XQ He, Y Huang, KC Hwang, “Failure analysis and the optimal toughness design of carbon nanotube-reinforced composites,” Composites Science and Technology, vol. 70, pp.1360-1367, 2010.

[8] YL Chen, B Liu, XQ He, Y Huang, KC Hwang, “Fracture Toughness of Carbon Nanotube-Reinforced Metal- and Ceramic-Matrix Composites,” Journal of Nanomaterials, vol. 2011, pp. 1-9, 2010.

[9] S kirtania, DChakraborty. “Multi-scale modeling of carbon nanotube reinforced composites with a fiber break.” Materials and Design, vol. 35, pp. 498-504. 2012.